DEVICE PERFORMANCES AND SIMULATIONS FOR SEVERAL KINDS OF LARGE-SCALE THIN FILM SILICON SOLAR CELL MODULES
-INTRODUCTION OF SUPER SEE-THROUGH THIN FILM SOLAR CELL MODULE AND APPLICATIONS

Katsushi Kishimoto, Yasushi Fujioka, Katsuhiko Nomoto, Akira Shimizu, and Toru Takeda
SHARP Corporation, 282-1 Hajikami, Katsuragi, Nara 639-2198, Japan, email: kishimoto.katsushi@sharp.co.jp
Phone: +81-745-63-3245 Fax: +81-745-63-3167

ABSTRACT: We fabricated large-scale thin film silicon solar cell modules with amorphous silicon and micro-crystallized p-i-n structure on a TCO film by a PECVD system. We also developed the device simulator for conventional and see-through thin film solar cell modules, and simulated their cell performances in order to estimate the influences of some electrical factors such as a series resistance, a shunt pass and its distribution. We confirmed the initial conversion efficiency of 12.1%(Pm 58.4W, Im 1.22A, Voc 67.4V, F.F. 0.711), corresponding to about 11% stabilized conversion efficiency and the initial conversion efficiency of 10.0%(Pm 48.1W, Im 1.05A, Voc 66.4V, F.F. 0.717) of a super see-through thin film solar module with 10% transparency with the same substrate size of 560x925mm.
Keywords: a-Si, Deposition, Micro Crystalline Si, Multijunction Solar Cell, PECVD, Simulation, Tandem

1 PURPOSE OF THIS WORK

Photovoltaic solar energy is becoming more and more important with the Kyoto environment coming pact into effect. And it is the key issues to improve the performances of thin film solar cells and applications in the market, because of strong demand from the market, especially in Europe. Recently, our company announced several kinds of new product with thin film solar cell modules, for example a super see-through solar cell modules and Lumiwall etc. We are going to apply the module for a sunroof, a marquee and illumination. We believe that these are opening the doors of the new category of solar energy market. Now, we are approaching to improve our technology for mass production for various kinds of thin film solar cell modules for the new market.

In this work, we explain our original technology, simulation method and our device performances for some kinds of large-scale thin film solar cell modules with a substrate size of 560x925mm.

2 EXPERIMENTS

We fabricated large-scale thin film silicon solar cells with amorphous silicon and micro-crystallized p-i-n structure on TCO film by the PECVD system. Our original technology about controlling short-pulsed generated VHF plasma[1], high transparent and conductive window layer of wide-gap p type a-Si film for a-Si solar cells[2] and a high transparent and conductive textured TCO films[3] have been reported so far. A novel growth technology of microcrystalline silicon thin films has been developed using short-pulsed VHF plasma CVD method[4].

Using several original methods for high efficiency and reliability of large-scale thin film solar cell modules with a substrate size of 560x925mm, we fabricated various kinds of the module. Compared with a conventional a-Si single junction module, the module was designed a fewer number of unit cells, because of higher voltage and lower current of each unit cell. A-Si:H and μc-Si:H films were deposited in a PECVD system. Rear electrode was sputtered by in-line DC sputtering system.

The structure of the cell was glass substrate / TCO / a-Si:H pin / μc-Si:H pin / rear electrode. After each principal deposition and sputtering, some integration processes by several laser patterning were done between each deposition. After connecting the lead wires on both sides of the module for collecting electricity generated by photon carriers in the area of the module, I-V characteristics of these modules were measured by a solar simulator with four Xenon lumps. Area distribution of light intensity with the solar simulator is ±2%, which conforms to the class A under JIS C 8933.

Some modules were prepared by super see-through treatments using a YAG laser, after ordinary cell fabrication process. The line width of a laser, which is scribing for the see-through area, was selected less than 200μm adequately, unless the stripes of the module by scribing see-through lines stand out outdoors under strong sunlight. Transparencies of these modules were easily adjusted to between 10 and 20% under visible light by changing the density of scribed lines in the module area.

We also simulated these cell performances using our device simulator for a large-scale thin film solar cell module in order to estimate the influences of some factors such as a series resistance, a shunt pass and its distribution. Outline of the device simulator is shown in Figure 1. At first, we calculated the I-V characteristics of the unit cell in a virtual module, which were obtained from the cell performances of test segments of 1x1cm at A.M.1.5 illumination. Next, both a series resistance and a shunt resistance of the cell in the module were calculated from its distributed I-V characteristics of each unit cell. Then, we obtained the I-V characteristics of the module, considering the influences of these resistance distributions in the module. We also estimated the influences of several cell parameters caused by material properties of each film against the module performance by using this simulator.

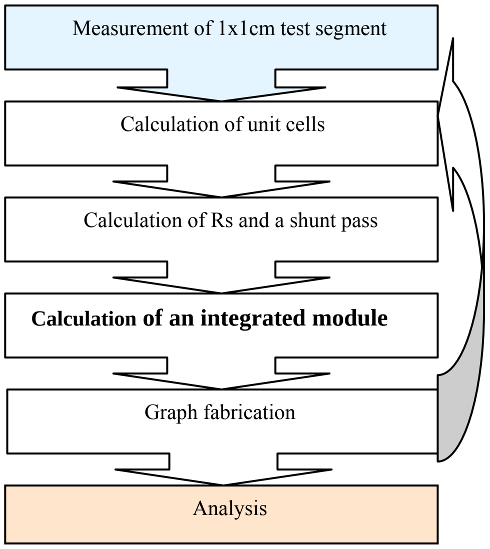

Figure 1: Schematic diagram of an outline of our device simulator for a large-area thin film solar cell module

Concerning about see-through cell structure, we also estimated the influence of both a series resistance and a shunt pass against the unit cell performance by the simulator. Figure 2 shows schematic diagram of (a) a large area conventional cell module, and (b) a large area see-through cell module. Compared with that of a conventional module, each unit cell's rear electrode of the see-through module is isolated. We estimated two kinds of cell structure, whose surface TCO film were with or without scribing on see-through lines. With TCO scribing on the lines, the unit cells on the same belt are completely isolated and series connected to the unit cells on the neighbor belts. Without TCO scribing, the unit cells on the same belt are parallel connected to each other and series connected to the unit cells on the neighbor belts. Blank arrows show the flow of a photocurrent.

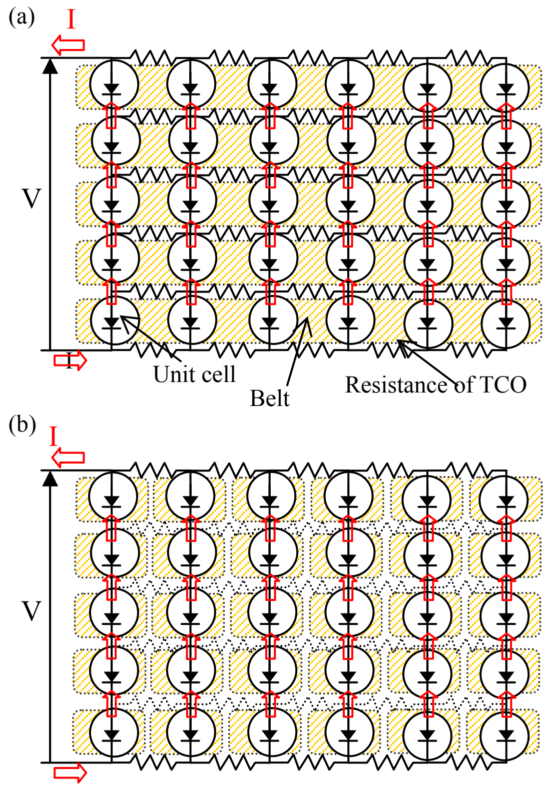

Figure 2: Schematic diagram of (a) a conventional solar cell module and (b) a see-through solar cell module

3 RESULTS

3.1 Uniformity of μc-Si film and cell performance

For making good use of high performances of the cells in the module, it is very important to improve the uniformity of the unit cell performances in the modules. Especially, the influence of the uniformity of device performances become severer in the case of the of tandem solar cell structure. The uniformity of the film thickness and the homogeneity of crystallinity in the area of a deposited Si film have been achieved by the short-pulsed VHF plasma method. Figure 3 illustrates (a) schematic diagram of each sample position in deposition area, and (b) comparison of crystallinity of intrinsic μ c-Si films between with continuous wave(C.W.) and with short-pulsed plasma. Crystallinity of the films were evaluated by the quotient of the intensity of μc-Si peak (Ic at about 520nm^{-1}) over that of a-Si peak(Ia at about 480nm^{-1}) which were measured by Raman spectroscopy. The values of Ic/Ia were distributed between 3.7 and 8.9 with C.W.. With a short-pulsed plasma, the values of Ic/Ia were between 4.5 and 6.2, whose distribution was reduced to about one-third of the films with a C.W. plasma.

(a)

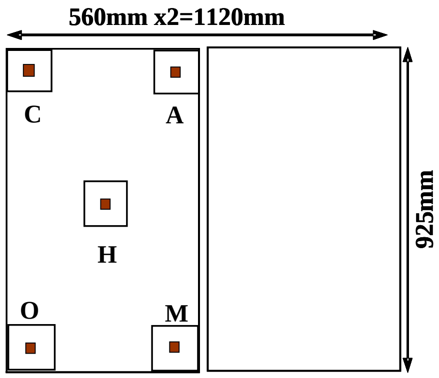

(b)

Position	Ic/Ia C.W.	Ic/Ia short-pulsed
A	5.6	4.5
C	4.1	4.5
H	8.9	6.2
M	3.7	5.7
O	5.1	5
Average	5.5	5.2
(Max-Min) /(Max+Min)	±41.3%	**±15.9%**

Figure 3: (a) Schematic diagram of each sample position in deposition area, and (b) Comparison of crystallinity of intrinsic μc-Si films with between C.W. and short-pulsed plasma

I layer		Jsc (mA/cm^2)	Voc (V)	F.F.	Eff. (%)
C.W.	Average	21.6	0.492	0.696	7.42
	Distribution	±10.0%	±7.1%	±5.6%	±16.8%
Short -pulsed	Average	**23.0**	**0.490**	**0.688**	**7.77**
	Distribution	**±4.1%**	**±4.2%**	**±2.7%**	**±8.0%**

Table Ⅰ: Comparison of I-V characteristics of 1x1 cm test segments between with C.W. plasma and with short-pulsed plasma

Table Ⅰ is the comparison of I-V characteristics of small test segments with between C.W. and short-pulsed VHF plasma. Both the distribution and average value with short-pulsed plasma were more improved than those with C.W. plasma. In both cases of film and cell preparation, the distributions had been much improved by short-pulsed VHF plasma. However, conversion efficiency of the cell has not been improved sufficiently. It is important to under long wavelength. Figure 4 illustrates spectra responses of a-Si(▲), μc-Si(◆) and c-Si cell(■) under A.M.1.5 illumination. Though the spectral response of μc-Si cell over 550nm is better than that of a-Si cell, it is possible for that of μc-Si cell to be more improved toward that of c-Si cell over the range of 800nm by improving film properties of I layer.

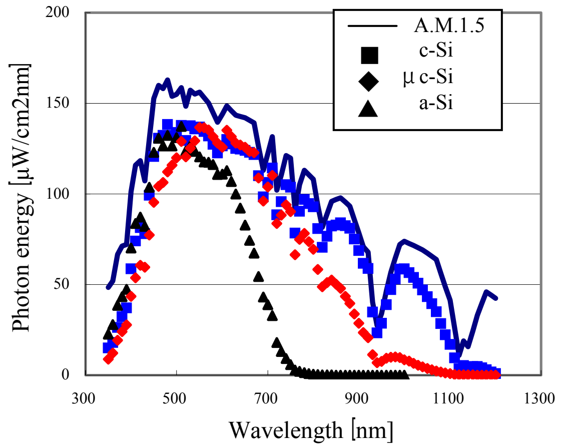

Figure 4: Comparison of spectral responses of a-Si(▲)and μc-Si(◆) with c-Si cell(■) under A.M.1.5 illumination

Figure 5 shows the comparison of a normalized output histogram of 1x1cm sample segments with between C.W. and short-pulsed plasma on a substrate size of 560mm x 925mm. The distribution under short-pulsed plasma condition does not only decrease abruptly, but also both the average and the peak value sift better than that of C.W. condition. These improvements with short-pulsed plasma are due to the better uniformities of μc-Si films.

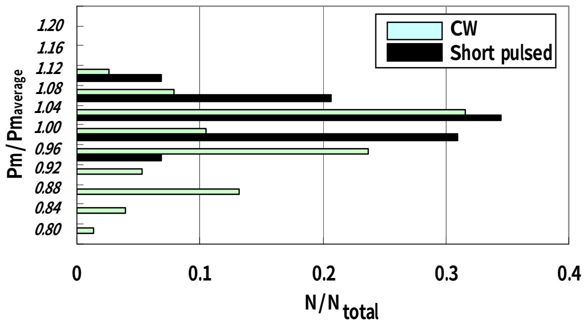

Figure 5: Comparison of a normalized output histogram of 1x1cm sample segments with between C.W. and short-pulsed plasma on the substrate size of 560mm x 925mm

3.2 Estimation of light induced degradation

Concerning about light induced degradation of the module under A.M.1.5 illumination, we evaluated several test segments of 1x1cm with same recipe of PECVD system. Figure 6 shows the time dependence of each normalized cell characteristics, for example normalized fill factor (F.F./F.F.0) and normalized conversion efficiency (η/η0), of a typical test segment under A.M.1.5 illumination. Jsc0, Voc0, F.F.0 and η0 mean the initial values of each cell parameter of the same test segment. Short circuit current (Jsc) and open circuit voltage (Voc) were almost stable over 1000 hours illumination, while F.F. degraded rapidly till 100 hours illumination and then stabilized at the point of 0.92 over 1000 hours illumination. In conclusion, light induced degradation of the cell strongly depends on only fill factor behavior. Then we estimated that the degradation ratio of the module is less than 10% under A.M.1.5 illumination.

3.3 Device simulator for a large-scale thin film solar module

We developed the device simulator for a large-scale solar cell module in order to estimate the influences of some factor (series resistance, shunt pass and distribution) and improve its performances. At first, under this good uniformity of each device parameter in the module area in Figure 3, we estimated the influences of both a resistance of TCO films and a shunt pass on device performance in the case of conventional module. Figure 7 shows the conversion efficiency and fill factor dependences on a resistance of TCO film or a shunt pass of the cell. In the case of conventional module, we found that it is much more important for the development of large area solar cell modules to reduce a series resistance, for example a resistance of TCO film, than to reduce power losses due to shunt passes for a large-scale thin film solar module. Next, we estimated the influences of both a resistance of TCO films and a shunt pass on device performance in the case of a see-through module. We compared a cell structure of TCO film scribing on see-through lines with that without TCO film scribing in order to select a proper see-through cell structure. However, even in the case of worse distribution of unit cell performances than that in Fig.2 on the simulation, the difference between with and without TCO scribing on see-through lines was unclear. We found that the see-through structure of a large-area thin film module both with and without TCO scribing weaken the influence of the distribution of the cell performance from the results of the simulation.

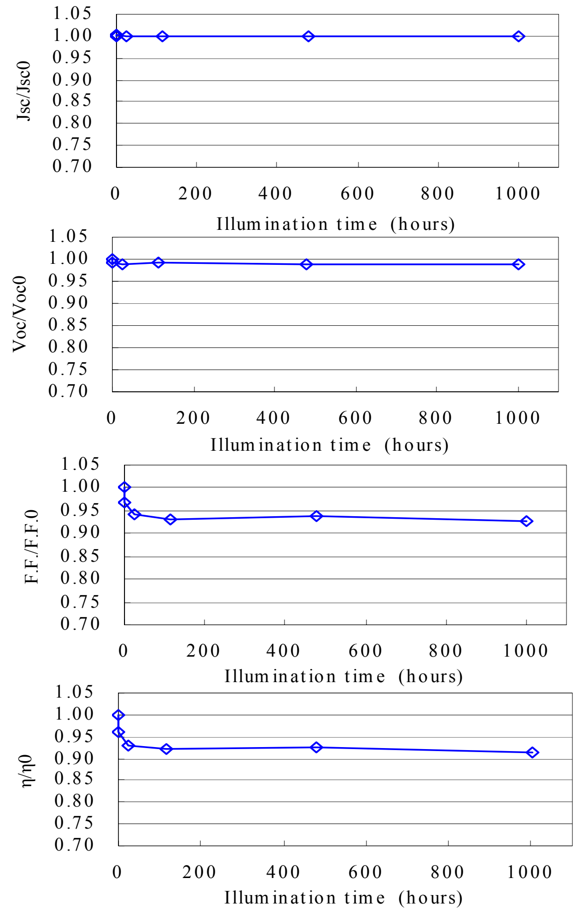

Figure 6: Time dependence of each normalized cell characteristics at A.M.1.5 illumination

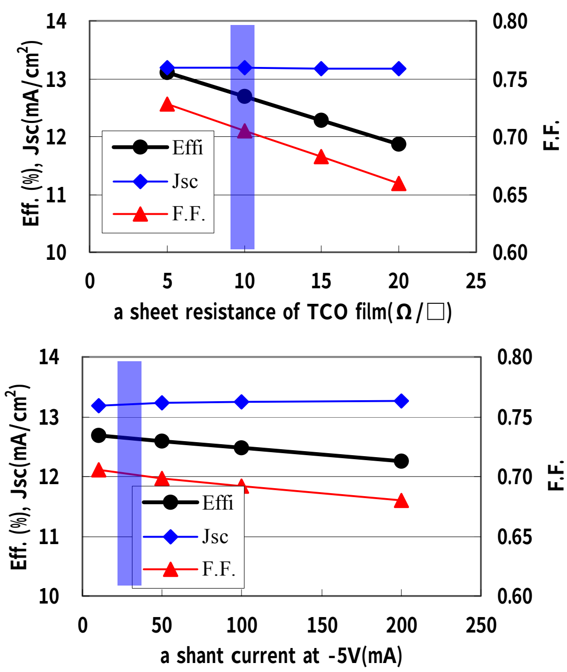

Figure 7: Conversion efficiency(Eff.) and fill factor(F.F.) dependences on a resistance of TCO film or a shunt pass of the cell(is the area of the present condition.)

3.4 I-V characteristics with a large-scale substrate size of 560x925mm

We fabricated several kinds of large-scale thin film silicon solar cell module with amorphous silicon and micro-crystallized p-i-n structure on a TCO film. As a result, we confirmed the initial conversion efficiency of 12.1% (Pm 58.4W, Im 1.22A, Voc 67.4V, F.F. 0.711) of a conventional module with a large-scale substrate size of 560x925mm, corresponding to about 11% stabilized conversion efficiency by short-pulsed plasma as is shown in Figure 8.

We also confirmed the initial conversion efficiency of 10.0% (Pm 48.1W, Im 1.05A, Voc 66.4V, F.F. 0.717) of a super see-through thin film solar cell module with 10% transparency, corresponding to about 9.2% stabilized conversion efficiency with a substrate size of 560x925mm as is shown in Figure 9. Considering about the reduction of effective area ratio in the module by see-through process, stabilized conversion efficiency in the effective area was equal to 10.1%. Normalized histogram of 100 sheets of large area cell module I-V characteristics is shown in Figure 10. Compared with that of conventional modules, although the distribution slightly increases, the peak sifts better. These results agree with our simulation calculations. At the same time our super see-through process is sufficiently reliable for the production of a large-scale module.

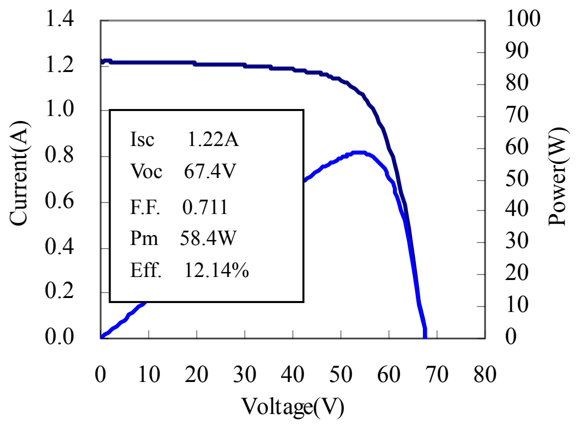

Figure 8: Initial I-V characteristics of a conventional thin film solar cell module

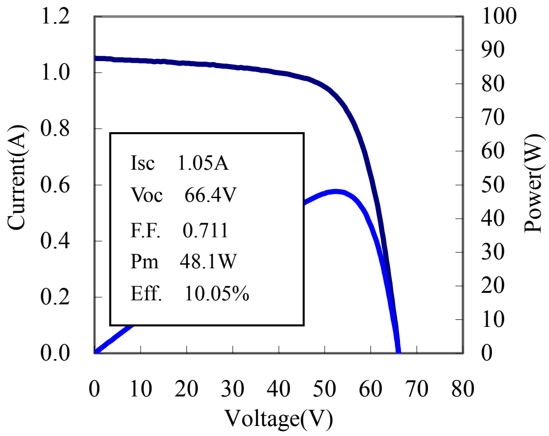

Figure 9: Initial I-V characteristics of a super see-through solar cell module with 10% transparency

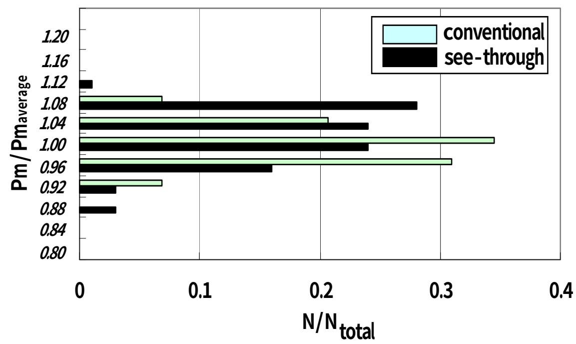

Figure 10: Comparison of a normalized output histogram with between conventional and super see-through modules on the substrate size of 560mm x 925mm

3.5 The external appearance of super solar cell modules

We can fabricate two sheets of super see-through solar cell module with different transparencies. Figure 11 shows the external appearance with a conventional thin film solar module and the super see-through solar cell modules with 10 and 20% transparency. Conventional module colors more black than a-Si module, because it has higher absorption of visible light as is shown in Figure 4. On the other hand, there is no remarkable difference between the module with 10% transparency and that with 20% transparency at a glance. Under strong light, we can easily see the landscape through the super see-through solar cell module with even 10% transparency as is shown in Figure 12. With 20% transparency, the side of back electrode became brighter than that with 10% transparency, so it was more inconspicuous and fitting into a transparent landscape.

Figure 11: The external appearance with a conventional thin film solar module and the super see-through solar cell modules with 10 and 20% transparency outdoors

Figure 12: The external appearance with a super see-through solar cell module with 10% transparency under strong light

4 CONCLUSIONS

We fabricated several kinds of large-scale thin film silicon solar cell module with amorphous silicon and micro-crystallized p-i-n structure on a TCO film.

・ In both cases of film and cell preparation, the distributions had been much improved by short-pulsed VHF plasma.

・ The see-through structure with a large-area thin film module weaken the influence of the distribution of the cell performance from the results of the simulation.

・ We also confirmed the initial conversion efficiency of 10.0% (Pm 48.1W, Im 1.05A, Voc 66.4V, F.F. 0.717) of a super see-through thin film solar cell module with 10% transparency, corresponding to about 9.2% stabilized conversion efficiency with a substrate size of 560x925mm.

Acknowledgements

The Authors are grateful to the other members of the same group for their help in the experiments.

REFERENCE

[1] K.Nomoto et al, 14th European PVSEC, 1997, pp.1226-1230

[2] K.Kishimoto et al, 11th PVSEC, 1999, pp.187-188

[3] K.Kishimoto et al, IEEE PVSC, 2000, pp.754-757

[4] Y.Fujioka et al, 14th PVSEC, 2004, pp.27-28